

Achievable Rate Region for Iterative Multi-User Detection via Low-cost Gaussian Approximation

Xiaojie Wang, *Student Member, IEEE*, Chulong Liang, Li Ping, *Fellow, IEEE*,
and Stephan ten Brink, *Senior Member, IEEE*

Abstract

We establish a multiuser extrinsic information transfer (EXIT) chart area theorem for the interleave-division multiple access (IDMA) scheme, a special form of superposition coding, in multiple access channels (MACs). A low-cost multi-user detection (MUD) based on the Gaussian approximation (GA) is assumed. The evolution of mean-square errors (MSE) of the GA-based MUD during iterative processing is studied. We show that the K -dimensional tuples formed by the MSEs of K users constitute a conservative vector field. The achievable rate is a potential function of this conservative field, so it is the integral along any path in the field with value of the integral solely determined by the two path terminals. Optimized codes can be found given the integration paths in the MSE fields by matching EXIT type functions. The above findings imply that i) low-cost GA detection can provide near capacity performance, ii) the sum-rate capacity can be achieved independently of the integration path in the MSE fields; and iii) the integration path can be an extra degree of freedom for code design.

Index Terms

EXIT chart, non-orthogonal multiple access, area theorem, MAC capacity.

Part of the results is to appear in the proceedings of the IEEE International Symposium on Information Theory 2019, Paris, France [1].

X. J. Wang and S. ten Brink are with Institute of Telecommunications, Pfaffenwaldring 47, University of Stuttgart, 70569 Stuttgart, Germany (e-mail: {wang, tenbrink}@inue.uni-stuttgart.de).

C. Liang and L. Ping are with the Department of Electronic Engineering, City University of Hong Kong, Hong Kong SAR, China (e-mail: {chuliang, eeliping}@cityu.edu.hk).

I. INTRODUCTION

Consider a multiple access channel (MAC) with K users. The MAC capacity region is bounded by $2^K - 1$ constraints and determined by a tuple of user rates R_k , $1 \leq k \leq K$ [2], [3]. To achieve arbitrary points of the capacity region, joint detection and decoding is required, which has prohibitively high complexity exponential to K . Theoretically, successive interference cancellation (SIC) together with time-sharing or rate-splitting can achieve the entire capacity region [4]. SIC involves subtraction of successfully detected signals. If practical forward error control (FEC) codes are used, each subtraction incurs an overhead in terms of either power or rate loss relative to an ideal capacity achieving code [5, Fig. 13.3]. Such overheads accumulate during SIC steps, moving its performance away from the capacity. Also, both time-sharing and rate-splitting involve segmenting a data frame of a user into several sub-frames. In practice, the length of a coding frame is restricted by the latency requirement. Frame segmentation results in shorter sub-frames and so reduced coding gain for a practical turbo or low-density parity-check (LDPC) type code [6], which further worsens the losses of accumulation.

Iterative detection [7]–[10] can alleviate the loss accumulation problem using soft cancellations instead of hard subtraction. A turbo or LDPC code involving iterative detection can be optimized by matching the so-called extrinsic information transfer (EXIT) functions of two local processors [11], [12]. In a single-user point-to-point channel, such matching can offer near capacity performance, as shown by the area properties [13], [14].

Interleave-division multiple-access (IDMA) is a low-cost transmission scheme for MACs [15]. A Gaussian approximation (GA) of cross-user interference is key to a low-cost IDMA detection technique. The per-user complexity of a GA-based MUD remains roughly the same for all K . For comparison, the complexity of a standard *a posteriori* probability (APP) based multi-user detector (MUD) is exponential in K [15].

A question naturally arises: At such low cost, what is the achievable performance of IDMA under GA-based MUD? Some partial answers to this question are available. It is shown that IDMA is capacity approaching when all users see the same channel [16]. However, for the general MAC system, the code design for IDMA becomes difficult when different users see different channels. In the latter case, to achieve the entire capacity region, different coding rates or different power levels are generally required. Previous works on IDMA focus on the achievability of some special points in the MAC capacity region [17]–[21] and/or other aspects, e.g., power control etc. [22]–[26]. To the best of our knowledge, no previous work has shown

that IDMA under the GA-based MUD can achieve the entire MAC capacity region.

This paper provides a comprehensive analysis of the achievable performance of IDMA under GA-based MUD. We approach the problem based on multi-dimensional curve matching. Let v_k be the mean-square error (MSE) (i.e., the variance) for the GA-based MUD for user k , with $v_k = 0$ indicating perfect decoding. Using the relationship between mutual information (MI) and minimum MSE (MMSE) derived in [14], [27], we show that the achievable sum-rate can be evaluated using a line integral along a valid path in the K -dimensional vector field $\mathbf{v} = [v_1, v_2, \dots, v_K]^T$. A main finding of this paper is that the integral is path-independent and its value is solely determined by the two terminations. The path independence property greatly simplifies the code optimization problem.

The contributions of this paper are summarized as follows.

- A low-cost GA-based MUD can provide near optimal performance. In particular, it is provably capacity-achieving for Gaussian signaling.
- Relative to Gaussian signaling, the loss due to finite modulation can be made arbitrarily small using a superposition coded modulation (SCM) technique.
- FEC codes optimized for single-user channels may not be good choices for MACs. The FEC codes should be carefully designed to match MUD, which facilitates iterative detection. We will provide examples for the related code design.
- A multi-user area theorem of EXIT chart is established for the code design. We show that the sum-rate capacity is a potential function in the MSE field formed by \mathbf{v} , which leads to the path independence property. All points of the MAC capacity region are achievable using only one FEC code per user. This avoids the loss related to the frame segmentation of SIC as aforementioned.
- The above results can be extended to MIMO MAC channels straightforwardly. We will provide simulation results to show that properly designed IDMA can approach the sum-rate MAC capacity for different decoding paths in the MSE field within 1 dB .

This paper is structured as follows. In Sec. II, we present the multiuser iterative detection and decoding scheme in IDMA along with the matching condition. Then, we derive the achievable rates of IDMA and show its implication in code design in single antenna setup in Sec. III. The achievable rate analysis is further extend to MIMO cases in Sec. IV. Sec. V provides code design examples and numerical results verifying our theorems. Finally, Sec. VI concludes the paper.

II. ITERATIVE IDMA RECEIVER

Consider a general K -user MAC system, which is described by

$$y = \sum_{k=1}^K \sqrt{P_k} h_k x_k + n \quad (1)$$

where P_k denotes the received signal strength of the k th user's signal, h_k denotes the fading coefficients of the user, x_k is the k th transmit signal and n is the additive (circularly symmetric complex) white Gaussian noise (AWGN) with zero mean and unit variance, i.e., $\mathcal{CN}(0, \sigma^2 = 1)$. We consider complex-valued signals throughout the paper if not otherwise stated. Practically, a sequence of symbols y , forming one or multiple codewords \mathbf{y} , is received.

The iterative receiver is depicted in Fig. 1. The elementary signal estimator (ESE) module has

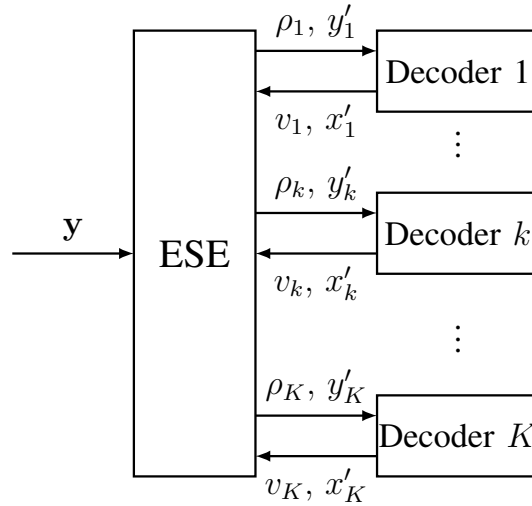


Fig. 1. The iterative multi-user detection and decoding model in IDMA.

access to the channel observation y and feedbacks x'_k from all the users' decoders. It performs the so called soft interference cancellation (SoIC) and output signals with reduced interference. Each decoder (DEC) performs decoding for a particular user while treating the residual signals of other users as noise. Through the iterative message passing between the ESE and DEC's, the wanted signals are refined and interference suppressed progressively. More details on the ESE DEC's are given below. For convenience of discussions, we will assume that x_i are modulated using binary phase shift keying (BPSK).

A. ESE functions

The function of the ESE (for elementary signal estimation) module in Fig. 1 is interference cancellation. The outputs of ESE are a sequence of y_k with

$$y_k = y - \tilde{z}_k = \sqrt{P_k} h_k x_k + z_k \quad (2a)$$

$$z_k = \sum_{i=1, i \neq k}^K \sqrt{P_i} h_i (x_i - \hat{x}_i) + n. \quad (2b)$$

Here, y_k is obtained from y in (1) by canceling out the mean of the interference $\tilde{z}_k = \sum_{i=1, i \neq k}^K \sqrt{P_i} h_i \hat{x}_i$ based on the feedback of the channel decoders. The soft symbol estimates \hat{x}_i are generated by feedbacks from the users' channel decoders. For instance with BPSK signaling, $\hat{x}_i = \tanh\left(\frac{L_i}{2}\right)$ with L_i being the log-likelihood ratio (LLR) after decoding. For higher modulation schemes, the soft symbol estimates can be obtained by [28, eqn. 3a]. The feedback from channel decoders will be discussed later in Sec. II-B. The term z_k in (2b) is comprised of AWGN and residual multi-user interference. To reduce complexity, we will adopt a Gaussian approximation (GA) assuming that z_k is Gaussian-distributed with zero mean and variance $\sigma_{z,k}^2$, i.e., $\mathcal{CN}(0, \sigma_{z,k}^2)$ ¹. From (2b), we obtain

$$\sigma_{z,k}^2 = \sum_{i=1, i \neq k}^K P_i |h_i|^2 v_i + \sigma^2 \quad (3a)$$

where the MSE of the symbol estimates $v_i = \mathbb{E}[|x_i - \hat{x}_i|^2]$ is to characterize the quality of the decoder feedback \hat{x}_i . The complexity in (3a) can be reduced by a sum-and-minus trick by noting that $\tilde{z}_k = \Sigma - \sqrt{P_k} h_k \hat{x}_k$ where $\Sigma = \sum_{i=1}^K \sqrt{P_i} h_i \hat{x}_i$. Here Σ is common to all users, so its cost can be shared. The per user cost for (3a) thus does not grow with K . The quality of the ESE output for user k can be measured by the signal-to-noise ratio (SNR) offered by y_k in (3a)

$$\rho_k = \frac{P_k |h_k|^2}{\sigma_{z,k}^2} = \frac{P_k |h_k|^2}{\sum_{i=1, i \neq k}^K P_i |h_i|^2 v_i + \sigma^2}, \quad \forall k = 1, 2, \dots, K. \quad (3b)$$

Assume that the average power of x_i is normalized to 1. Then $v_i = 1$ in the first iteration, meaning no a prior information about x_i . During the iterative detection, v_i will be updated using

¹The Gaussian assumption is valid for a large number of users with arbitrary independently transmitted symbols x_i as the consequence of the central limit theorem or if the transmit signals x_i are Gaussian by themselves.

decoder output (See the discussion in Sec. II-B below). For K users, we express (3b) in a vector form as

$$\boldsymbol{\rho} = \phi(\mathbf{v}) \quad (3c)$$

where $\boldsymbol{\rho} = [\rho_1, \rho_2, \dots, \rho_K]^T$ and $\mathbf{v} = [v_1, v_2, \dots, v_K]^T$. Due to the fact that the MSE is bounded by $0 \leq v_i \leq \mathbb{E}[|x_i|^2] = 1$, we obtain that the SNR is also bounded by

$$\rho_{k,\min} = \frac{P_k |h_k|^2}{\sum_{i=1, i \neq k}^K P_i |h_i|^2 + \sigma^2} \leq \rho_k \leq \frac{P_k |h_k|^2}{\sigma^2} = \rho_{k,\max}. \quad (3d)$$

We will view (3) as a transfer function from \mathbf{v} to $\boldsymbol{\rho}$.

B. DEC functions

The refined signals y_k in (2) generated by the ESE are forwarded to the DEC. The latter consists of K local decoders (DECs, see Fig. 1) performing extrinsic decoding based on y_k with SNR ρ_k . To reduce complexity, we will adopt a Gaussian approximation (GA) that z_k is Gaussian-distributed with zero mean and variance $\sigma_{z,k}^2$. Then the standard decoding operations [6], [12] can be applied to the local decoders. The outputs of an APP decoder are extrinsic messages that are assumed to resemble observations from the AWGN channel, i.e.,

$$x'_k = x_k + w_k \quad (4)$$

where w_k follows a Gaussian-distribution $\mathcal{CN}(0, \sigma_{w,k}^2)$. Let the MSEs for \hat{x}_k be v_k after decoding. The MSEs v_k are also the MMSE of the conditional mean estimator due to APP decoding, thus, we define a transfer function for DEC k as

$$v_k = \mathbb{E}[|x_k - \mathbb{E}[x_k | x'_k]|^2] = \psi_k(\rho_k), 0 \leq v_k \leq 1, \forall k = 1, 2, \dots, K. \quad (5a)$$

Or in a vector form for the overall DEC

$$\mathbf{v} = \psi(\boldsymbol{\rho}). \quad (5b)$$

In general, unlike $\phi(\cdot)$ in (3c), we do not have an explicit expression for $\psi(\cdot)$ in (5b), but it can be numerically measured. The details can be found in [29].

In general, $\psi_k(\rho_k)$ can be

$$v_k = \begin{cases} 1, & \rho \leq \rho_{k,\min} \\ \psi_k(\rho_k), & \rho_{k,\max} \leq \rho \leq \rho_{k,\min} \\ 0 & \rho \geq \rho_{k,\max} \end{cases} \quad (5c)$$

Here the first case of $v_k = 1$ is for the boundary condition $\rho \leq \rho_{k,\min}$ in (3d) at the start of the iterative detection. On the other hand, the last case of $v_k = 0$ is for the boundary condition $\rho \geq \rho_{k,\max}$ in (3d) at the end of the iterative detection when all interference has been perfectly canceled out and perfect decoding is assumed to be achievable at this point.

To track the convergence behavior of the iterations between ESE and DEC, we write the SNR $\boldsymbol{\rho}$ and MSE \mathbf{v} vector as functions of an iteration variable t as

$$\mathbf{v} = \mathbf{v}(t) \quad \text{and} \quad \boldsymbol{\rho} = \boldsymbol{\rho}(t) \quad (5d)$$

Let t_0 and t_∞ denote the start and end of the iterative processing, we require that

$$\mathbf{v}(t_0) = \psi(\boldsymbol{\rho}(t_0)) = \mathbf{1} \quad (5e)$$

$$\mathbf{v}(t_\infty) = \psi(\boldsymbol{\rho}(t_\infty)) = \mathbf{0} \quad (5f)$$

since we are interested in the error-free decoding cases.

C. Matching condition

We will say that the ESE and DEC functions are matched if the following condition is met

$$\psi(\boldsymbol{\rho}(t)) = \phi^{-1}(\boldsymbol{\rho}(t)). \quad (6)$$

Note that the matching condition in (6) is along a K -dimensional line given by $\boldsymbol{\rho}(t)$. It is not required to match $\psi(\boldsymbol{\rho})$ and $\phi(\boldsymbol{\rho})$ in the entire K dimensional space, i.e., requiring $\psi(\boldsymbol{\rho}) = \phi^{-1}(\boldsymbol{\rho})$. The line matching in (6) is much easier. We will show that such line matching achieves the MAC capacity (see Sec. III-A).

III. ACHIEVABLE RATES

The fundamental relation between achievable rate and MMSE in AWGN channels $y = x + n$ is found by Guo et. al. [27] as

$$R(\text{snr}) = \int_0^{\text{snr}} \text{mmse}(\rho) d\rho.$$

for any input distribution of x . The above result is extended to iterative decoding in [14]. Following [14] and also [27], [28], the achievable rate for user k using GA-based MUD is given by

$$R_k = \int_0^\infty f(\rho_k + f^{-1}(v_k)) d\rho_k, \quad \forall k = 1, 2, \dots, K. \quad (7)$$

where $f(\rho) = v$ is the achievable MMSE for a given constellation of x by observing y at the SNR of ρ . Intuitively, ρ_k and $f^{-1}(v_k)$ give, respectively, the SNRs related to the input and extrinsic messages of the k th DEC. Hence $\rho_k + f^{-1}(v_k)$ represents the overall SNR after combining these two messages.

A. Gaussian alphabets

We first consider the case when x_i are Gaussian distributed. This can be approximated by using e.g., superposition coded modulation (SCM) [30], [31]. The MMSE for Gaussian signals is given by $f(\rho) = \frac{1}{1+\rho}$, and with (7) the achievable rates can be expressed as

$$R_k = \int_0^\infty \frac{1}{\rho_k(t) + v_k^{-1}(t)} d\rho_k(t), \quad \forall k = 1, 2, \dots, K. \quad (7a)$$

Here $v_k(t)$ and $\rho_k(t)$ are related by the function in (3b) and (5), and they are expressed as the functions of t , as introduced in (5d). In Appendix A, we will consider (3b) and (5) and rewrite (7a) into the following form:

$$R_k = - \int_{v_k=1}^{v_k=0} \frac{g_k}{\sum_{i=1}^K g_i v_i(t) + \sigma^2} dv_k(t) = - \int_{v_k=1}^{v_k=0} \frac{g_k}{\mathbf{g}^T \mathbf{v}(t) + \sigma^2} dv_k(t) \quad \forall k = 1, 2, \dots, K \quad (7b)$$

where $\mathbf{g}^T = [P_1 |h_1|^2, P_2 |h_2|^2, \dots, P_K |h_K|^2]^T$ contains the powers of all users, $\mathbf{v} = [v_1, v_2, \dots, v_K]^T$ and $g_k = P_k |h_k|^2$ denotes the k th element of vector \mathbf{g} . Note that the achievable rate expression in (7b) depends on multiple variables v_1, v_2, \dots and v_K , i.e., the evolution of the MSEs of all the DECs. This can be intuitively explained by the iterative soft interference cancellation of the ESE based on other users' DEC feedbacks.

Hence, the achievable sum-rate of all users can be written as

$$R_{\text{sum}} = \sum_{k=1}^K R_k = - \int_{\mathbf{v}(t)} \frac{\mathbf{g}}{\mathbf{g}^T \mathbf{v}(t) + \sigma^2} \cdot d\mathbf{v}(t) \quad (8a)$$

where (8a) denotes a line integral defined by $\mathbf{v}(t)$, $t \in [t_0, t_\infty]$. Notice that the line $\mathbf{v}(t)$ is determined by the evolution of the MSE vector \mathbf{v} of all DECs. We recall that the terminals of the line are given in (5e) and (5f) as $\mathbf{v}(t_0) = \mathbf{1}$ and $\mathbf{v}(t_\infty) = \mathbf{0}$. It can be verified that the integrands

constitute a gradient of a scalar field (or potential function), i.e., $\frac{\mathbf{g}}{\mathbf{g}^T \mathbf{v} + \sigma^2} = \nabla_{\mathbf{v}} \log(\sigma^2 + \mathbf{g}^T \mathbf{v})$. Thus, the achievable sum-rate can be written as

$$\begin{aligned} R_{\text{sum}} &= - \int_{L=\mathbf{v}(t)} [\nabla \log(\sigma^2 + \mathbf{g}^T \mathbf{v})] \mathbf{v}'(t) dt \\ &= \log \left(\frac{\sigma^2 + \mathbf{g}^T \mathbf{v}(t_0)}{\sigma^2 + \mathbf{g}^T \mathbf{v}(t_\infty)} \right) \\ &\stackrel{(5e),(5f)}{=} \log \left(1 + \frac{\sum_{k=1}^K P_k |h_k|^2}{\sigma^2} \right) \end{aligned} \quad (8b)$$

which is independent of the path taken for the integration. We note that the achievable rate in (8b) coincides with the multi-user Shannon capacity. In other words, any path with matched DEC functions can achieve the multi-user Shannon capacity. Therefore, the matching condition given in (6) is a sufficient condition for achieving the sum-rate capacity. It can be further verified that the matching condition also constitutes a necessary condition for achieving the multi-user Shannon capacity. Consider the case $\mathbf{v}(t) < \phi^{-1}(\boldsymbol{\rho}(t))$, then we have $R_k < - \int_{v_k=1}^{v_k=0} \frac{g_k}{\mathbf{g}^T \mathbf{v} + \sigma^2} dv_k$ and thus $R_{\text{sum}} < \log \left(1 + \frac{\sum_{k=1}^K P_k |h_k|^2}{\sigma^2} \right)$. On the contrary, for the case $\psi(\boldsymbol{\rho}(t)) > \phi^{-1}(\boldsymbol{\rho}(t))$, error-free decoding is not possible.

This leads to the following theorem.

Theorem 1. *The achievable sum-rate in IDMA for any path $L(t) : \mathbf{v}_s = \mathbf{1} \rightarrow \mathbf{v}_e = \mathbf{0}$ (starting from $\mathbf{v}_s = \mathbf{1}$ to $\mathbf{v}_e = \mathbf{0}$) is given by the multiuser Shannon capacity*

$$\begin{aligned} R_{\text{sum}} &= - \int_{\mathbf{v}(t)} f(\boldsymbol{\rho}(t) + f^{-1}(\mathbf{v}(t))) \cdot d\boldsymbol{\rho}(t) \\ &= \log \left(1 + \frac{\sum_{k=1}^K P_k |h_k|^2}{\sigma^2} \right) \end{aligned}$$

with the following assumptions

- 1) *The exchanged messages during the iterative processing of the extrinsic and a priori channel are observations from AWGN channels, given in (3a) and (4).*
- 2) *The channel decoder is APP (i.e., MAP) decoder.*
- 3) *The channel encoders and decoders use “matched codes” for a given path in the MMSE-field given in (6).*

Remark: The assumptions used in Theorem 1 are common for turbo-type iterative receivers. It is generally accepted that these assumptions are sufficiently accurate for practical systems, based on which turbo and LDPC codes are designed in many modern communication systems

[11], [32]. Theorem 1 provides guidelines for the design of FEC codes in the matching condition discussed in Sec. II-C for multi-user scenarios. Further, various channel decoders such as BCJR and belief propagation (BP) are known for achieving APP performance.

B. Finite alphabets

If the symbols $x_i \in \mathcal{S}_i$ are taken from finite alphabets $|\mathcal{S}_i| < \infty$, the capacity formula, in general, can not be expressed in closed-form. Notice that eq. (7) is still valid, using the MMSE-formula for the underlying modulation format $f(\rho) = v$. It is also well known that the loss incurred by finite alphabets, compared with Gaussian, is negligible in the low-SNR regime. Besides, the Gaussian capacity can be approached by higher order modulations with shaping and/or SCM [30].

We provide in the following an achievable rate analysis for IDMA with quadrature phase shift keying (QPSK) signaling. The achievable sum-rate can be written as

$$R_{\text{sum}} = \int_{\boldsymbol{\rho}(t)} f_Q(\boldsymbol{\rho}(t) + f_Q^{-1}(\mathbf{v}(t))) d\boldsymbol{\rho}(t). \quad (9)$$

where $f_Q(\cdot)$ denotes the MMSE of QPSK, which is given by

$$f_Q(\rho) = 1 - \int_{-\infty}^{\infty} \tanh(\rho - y\sqrt{\rho}) \frac{e^{-\frac{y^2}{2}}}{\sqrt{2\pi}} dy. \quad (10)$$

In AWGN channels, Gaussian signals are the hardest to estimate [33], i.e.,

$$f_X(\rho) \leq f_G(\rho) = \frac{1}{1 + \rho}.$$

for any input distribution X with the same variance. Hence, the achievable rate with distributions other than Gaussian is essentially smaller.

Example: The users are assumed to have same power P and $h_k = 1$, $\forall k$, modulation and coding scheme. For simplicity, we define $t_0 = 0$ and $t_\infty = 1$ and consider the following integration path $\boldsymbol{\rho}(t)$

$$\boldsymbol{\rho}(t) = \frac{P}{(K-1)P + \sigma^2} \mathbf{1} + \left(\frac{P}{\sigma^2} - \frac{P}{(K-1)P + \sigma^2} \right) \cdot t \cdot \mathbf{1} \quad t \in [0, 1]$$

and with (3b)

$$\mathbf{v}(t) = \frac{(1-t)\sigma^2}{\sigma^2 + (K-1)P \cdot t} \cdot \mathbf{1}. \quad t \in [0, 1]$$

Then, the achievable rate can be numerically evaluated for the specified path. We compare the achievable rates using QPSK with different number of users in Fig. 2 by numerically solving

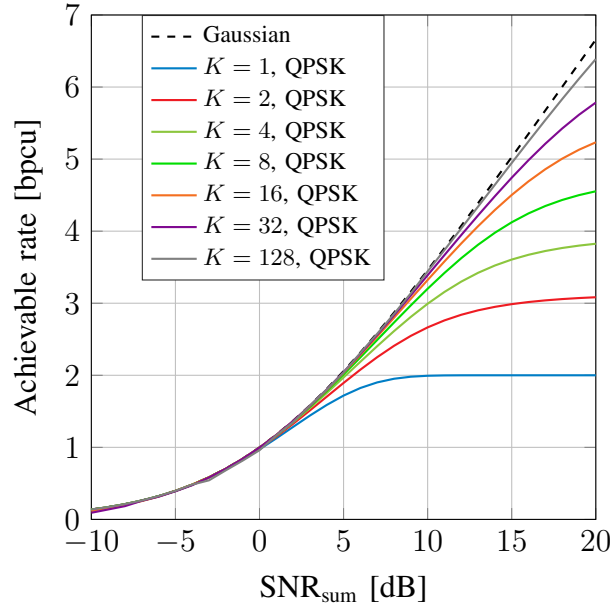


Fig. 2. Achievable rates of multiuser IDMA with matching codes and QPSK modulation; all users are assumed to have the same power, modulation and coding scheme; For fair comparison, the multi-user SNR $\text{SNR}_{\text{sum}} = KP/\sigma^2$ is used as abscissa.

the integral (9). Clearly, the loss to Gaussian capacity, due to finite modulation, can be made arbitrarily small by imposing a larger number of users or data layers (which may belong to a same user) into the system. Although we assumed equal-power and equal-rate for simplicity, the achievable rates analysis can be extended to other general cases straightforwardly.

We will provide code matching examples for a three user case based on QPSK signaling in Sec. V. The achievable rates can also be found by the density evolution (DE) method, which are very close to the Gaussian capacity.

C. Path vs rate tuples

Consider a simple two-user case, i.e., $K = 2$. Fig. 3 illustrates some special paths and their corresponding achievable rate tuple (or rate pair here). The simplest path is a straight line between the starting point $\mathbf{v}(t_0) = \mathbf{1}$ and the stop point $\mathbf{v}(t_\infty) = \mathbf{0}$, denoted by *path 1*. It is straightforward to obtain

$$R_k = \frac{g_k}{\mathbf{g}^T \mathbf{1}} \log \left(1 + \frac{\mathbf{g}^T \mathbf{1}}{\sigma^2} \right), \forall k = 1, 2, \dots, K.$$

In this case, the achievable rate of each user is proportional to the received signal power strength g_k . For the two-user case, this rate tuple coincides with the point where TDMA/FDMA achieves the sum-rate capacity (see green dot in Fig. 3). In *path 1*, it satisfies

$$v_1(t) = v_2(t) = \dots = v_K(t) = v(t), \forall t.$$

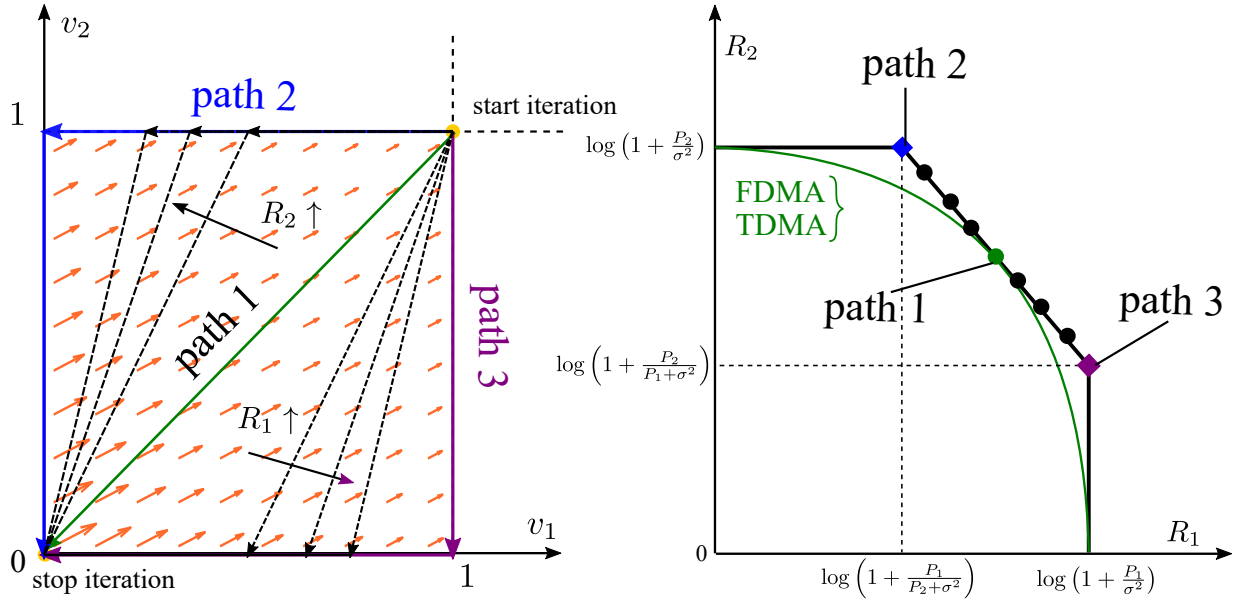


Fig. 3. Illustration (exemplary for two users) of different integration paths achieving different rate pairs (R_1, R_2) ; the arrows in the left figure illustrate the two-dimensional MSE vector field; the achieved rate pairs are marked in the right figure for the corresponding paths; the dashed lines denote paths achieving rate pairs moving (from the green dot) toward the corresponding SIC corner points.

The matching code for k th user shall have the following MSE characteristic function

$$v_k = \begin{cases} 1 & \rho_k \leq \rho_{k,\min} \\ \frac{1}{\mathbf{g}^T \mathbf{1} - g_k} \cdot \left(\frac{1}{\rho_k} - \sigma^2 \right) & \rho_{k,\min} \leq \rho_k \leq \rho_{k,\max} \\ 0 & \rho_k \geq \rho_{k,\max} \end{cases}.$$

For *path 2* and *path 3* which are comprised of K segments and each segment has merely value change (from $v_l = 1$ to $v_l = 0$) in one particular direction v_l , i.e., within the segment $\frac{dv_l}{dt} \neq 0$ and $\frac{dv_k}{dt} = 0, \forall k \neq l$. Depending on the order of the segments, there exist $K!$ such paths, which constitute the $K!$ SIC corner points of MAC capacity region. The user rate can be written as

$$R_k = \log \left(1 + \frac{g_k}{\sum_{l=\pi(k)+1}^K g_l + \sigma^2} \right), \forall k = 1, 2, \dots, K,$$

where $\pi(k) = k'$ denotes the permutation of user order with $1 \leq \pi(k) \leq K$ and $\pi(k) \neq \pi(k'), \forall k \neq k'$. The corresponding decoding functions are given by

$$v_k = \psi_k(\rho_k) = \begin{cases} 1 & \rho_k < \rho_{k,\text{SIC}} \\ 0 & \rho_k \geq \rho_{k,\text{SIC}} \end{cases}$$

where

$$\rho_{k,\text{SIC}} = \frac{g_k}{\sum_{l=\pi(k)+1}^K g_{\pi(l)} + \sigma^2}$$

are the decoding thresholds. The decoding functions are step functions with sharp transitions at corresponding threshold SNRs $\rho_{k,\text{SIC}}$. This type of decoding functions may pose difficulties for practical code designs, compared to that with smooth transitions.

D. Achievable rate region

To achieve an arbitrary point of the MAC capacity region, other paths shall be found. In the following theorem, we show that the entire MAC capacity region can be achieved by proving the existence of a dedicated path achieving an arbitrary point within the capacity region. Examples for constructing a dedicated path achieving a feasible rate tuple are provided in *case 2* of Sec. V-A.

Theorem 2. *Under the assumptions in Theorem 1, IDMA with GA-based MUD achieves every rate tuple in the K -user MAC capacity region $\mathcal{C}(K)$. Given a feasible target rate tuple $\mathbf{R} = [R_1, R_2, \dots, R_K] \in \mathcal{C}(K)$, there exists at least one path defined by $\mathbf{v}_R(t) : \mathbf{v}_s = \mathbf{1} \rightarrow \mathbf{v}_e = \mathbf{0}$ which achieves \mathbf{R} .*

Proof: See Appendix B. ■

Remark: It is easy to prove that there exists a unique path for each of the $K!$ SIC corner points and the decoding functions shall be step functions. For other rate tuples, it can be verified that there exist many different paths achieving that rate tuple. The choice of the integration path poses varying degrees of difficulty for the design of matching codes. Thus, the design of an appropriate integration path could be an extra degree of freedom for code design.

E. Gaussian Approximation

We provide in this section numerical evidence showing that the GA used in our achievable rate analysis is accurate enough for addressing the behavior of a practical iterative IDMA multiuser demodulator and decoder. The technique we used to track the probability density function (PDF) of the exchanged messages during the iterative processing is discretized density evolution (DDE) proposed in [34].

The GA is arguably true for large number of users (central limit theorem) and/or noise-limited scenarios (the noise density rather the multiple access interference governs the iterative process).

We verified the GA through DDE for these cases (results omitted). Instead, we show results for the following example with a few number of users operating at relatively high SNR, since the GA becomes skeptical in these cases.

Example: The number of users is set to $K = 4$, each with the same power $P = \frac{1}{4}$ and BPSK modulation. The multiuser SNR is $-10 \log \sigma^2 = 20$ dB. An LDPC code with the variable node degree profile (from “edge” perspective) $0.5231\lambda^1 + 0.3187\lambda^2 + 0.1582\lambda^{11}$ and the check node degree η^2 is used for each user. The PDF of Log-likelihood ratio (LLR) at the output of the LDPC variable node decoder (VND) is tracked using DDE with 10 bits and shown in Fig. 4 for the first 8 iterations. Clearly, the interference plus noise does not resemble a Gaussian density at

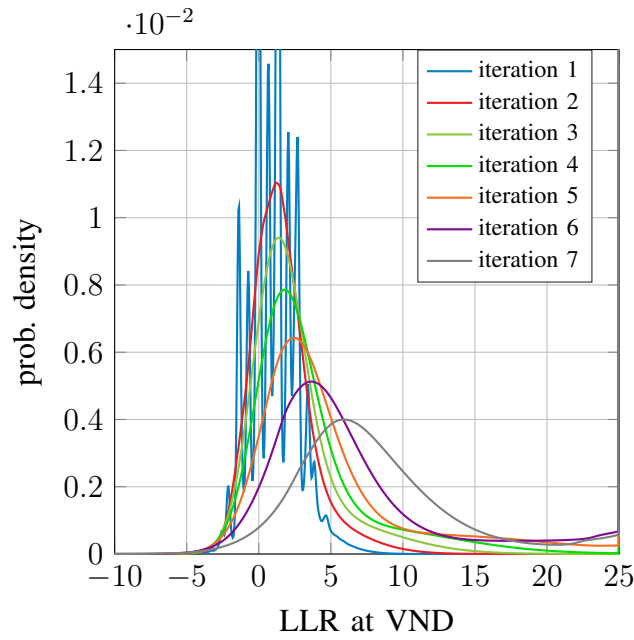


Fig. 4. LLR distribution at the VND during the iterative multiuser detection and decoding model with $K = 4$ users at the SNR of 20 dB; the symbol $x = +1$ is assumed to be transmitted for the user under test.

the first iteration. As the consequence of the soft interference cancellation, the density at VND becomes more Gaussian-like as the iteration proceeds. Similar trend can be observed also at the output of ESE and CND (results not shown). Surprisingly, the GA is quite accurate even for a few number of users operating at high SNR regime.

IV. MU-MIMO CHANNEL

Assume that the k th transmitter has $N_{t,k}$ antennas and the receiver has N_R antennas respectively; then, the received signal can be written as

$$\mathbf{y} = \sum_{k=1}^K \sqrt{P_k} \mathbf{H}_k \mathbf{x}_k + \mathbf{n} \quad (11)$$

where \mathbf{H}_k is the channel of the k th user, \mathbf{n} denotes the uncorrelated noise $\mathbb{E}[\mathbf{n}\mathbf{n}^H] = \sigma^2\mathbf{I}$. In this case, the ESE module is replaced by an iterative linear MMSE (LMMSE) receiver [28, eqn. (4a)]. Under the LMMSE-based ESE, the SNR of user k can be written as [35]

$$\rho_k = \frac{\sum_{i=1}^{N_{t,k}} \mathbf{h}_{k,i}^H \mathbf{R}^{-1} \mathbf{h}_{k,i}}{1 - v_k \sum_{i=1}^{N_{t,k}} \mathbf{h}_{k,i}^H \mathbf{R}^{-1} \mathbf{h}_{k,i}} \quad (12)$$

where $\mathbf{h}_{k,i}$ denotes the i th column of the k th user's channel matrix \mathbf{H}_k and

$$\mathbf{R} = \sigma_n^2 \mathbf{I} + \mathbf{H}\mathbf{V}\mathbf{H}^H$$

with $\mathbf{V} = \text{diag}(P_1 v_1, P_2 v_2, \dots, P_K v_K)$ and \mathbf{H} being the concatenated channels of all users. Following a similar approach in Appendix A, we obtain with the matching condition in (6) the user rate R_k as

$$R_k = \left[- \int \sum_{i=1}^{N_{t,k}} \mathbf{h}_{k,i}^H \mathbf{R}^{-1} \mathbf{h}_{k,i} dv_k \right]_{v_k=1}^{v_k=0}$$

Therefore, the sum-rate can be obtained as

$$\begin{aligned} R_{\text{sum}} &= \sum_{i=1}^K R_i = - \int_{\mathbf{v}=1}^{\mathbf{v}=0} \nabla \log \det [\mathbf{R}] d\mathbf{v} \\ &= \log \det \left[\mathbf{I} + \frac{1}{\sigma_n^2} \mathbf{H}^H \mathbf{P} \mathbf{H} \right] \end{aligned} \quad (13)$$

where $\mathbf{P} = \text{diag}(P_1, P_2, \dots, P_K)$. Path independence follows from the condition

$$\frac{\partial}{\partial v_k} \log \det [\mathbf{R}] = \text{trace} [\mathbf{R}^{-1} \mathbf{H}_k \mathbf{H}_k^H] = \sum_{i=1}^{N_{t,k}} \mathbf{h}_{k,i}^H \mathbf{R}^{-1} \mathbf{h}_{k,i}$$

with Jacobi's formula.

V. RESULTS

The code design for multi-user can be complicated [36]–[39]. For simplicity, we consider a single-input single-output (SISO) setup. We assume that the power levels $g_i = P_i |h_i|^2$ ($i = 1, \dots, K$) are constant in our code design. Thus, the multi-user SNR is defined as

$$\text{SNR}_{\text{sum}} = \frac{\sum_{i=1}^K g_i}{\sigma^2}. \quad (14)$$

We consider $K = 3$ users with the power distribution $\mathbf{g} = [g_1, g_2, g_3]^T = [\frac{1}{7}, \frac{2}{7}, \frac{4}{7}]^T$ and we target the sum-rate $R_{\text{sum}} = R_1 + R_2 + R_3 = 1$ bpcu as an example. Theoretically, this sum-rate

is attainable at the noise variance $\sigma^2 = 1$. Furthermore, the capacity region (more precisely, the *dominant face* which maximizes the sum-rate) with Gaussian alphabets is given by

$$\begin{aligned} 0.1069 &\leq R_1 \leq \log_2 \left(1 + \frac{g_1}{\sigma^2} \right) = 0.1926, \\ 0.2224 &\leq R_2 \leq \log_2 \left(1 + \frac{g_2}{\sigma^2} \right) = 0.3626, \\ 0.4854 &\leq R_3 \leq \log_2 \left(1 + \frac{g_3}{\sigma^2} \right) = 0.6521, \\ R_1 + R_2 &\leq \log_2 \left(1 + \frac{g_1 + g_2}{\sigma^2} \right) = 0.5145, \\ R_1 + R_3 &\leq \log_2 \left(1 + \frac{g_1 + g_3}{\sigma^2} \right) = 0.7776, \\ R_2 + R_3 &\leq \log_2 \left(1 + \frac{g_2 + g_3}{\sigma^2} \right) = 0.8931. \end{aligned}$$

A. ESE Functions

According to the matching condition in (6), for the design of capacity-achieving codes, the ESE transfer functions $\rho(t) = \phi(\mathbf{v}(t))$ shall be determined. For this, we specify the K -dimensional decoding path $\mathbf{v}(t)$.

As the path independence property of Theorem 1, we can constraint $\mathbf{v}(t)$ to be a piecewise linear path with n segments starting from the point $\mathbf{v}(t = 0) = \mathbf{x}_0 = \mathbf{1}$, crossing the intermediate points $\mathbf{v}(t = i) = \mathbf{x}_i = [x_{i,1}, \dots, x_{i,K}]^T, i = 1, 2, \dots, n-1$, and terminating at the point $\mathbf{v}(t = n) = \mathbf{x}_n = \mathbf{0}$, where $\mathbf{x}_i \neq \mathbf{x}_j, \forall i \neq j$ and for practical decoding

$$1 \geq x_{1,k} \geq x_{2,k} \geq \dots \geq x_{n-1,k} \geq 0 \forall k \quad (15)$$

shall apply. Therefore, the path can be expressed in a vector form as

$$\mathbf{v}(t) = \mathbf{x}_i - (\mathbf{x}_i - \mathbf{x}_{i+1}) \cdot (t - i), t \in [i, i + 1] \quad (16)$$

for $i = 0, 1, 2, \dots, n-1$. With the specified path, the ESE transfer function for user k can be computed as

$$\begin{aligned} \rho_k &= \phi_k(v_k) = \frac{g_k}{\mathbf{g}^T \mathbf{v}(t) - g_k v_k(t) + \sigma^2} \\ &= \frac{g_k}{\mathbf{g}^T \left[\mathbf{x}_i - (\mathbf{x}_i - \mathbf{x}_{i+1}) \cdot \frac{x_{i,k} - v_k}{x_{i,k} - x_{i+1,k}} \right] - g_k v_k + \sigma^2}, \\ &= \frac{g_k}{\sum_{k' \neq k}^K g_{k'} \left(\frac{x_{i,k'} - x_{i+1,k'}}{x_{i,k} - x_{i+1,k}} v_k + \frac{x_{i,k} x_{i+1,k'} - x_{i+1,k} x_{i,k'}}{x_{i,k} - x_{i+1,k}} \right) + \sigma^2}, \\ v_k &\in [x_{i+1,k}, x_{i,k}] \text{ for } i = 0, 1, 2, \dots, n-1. \end{aligned} \quad (17)$$

Note that when $x_{i,k} = x_{i+1,k}$, the above function is not valid. Actually, ρ_k is a vertical line from $\frac{g_k}{\mathbf{g}^T \mathbf{x}_i - g_k x_{i,k} + \sigma^2}$ to $\frac{g_k}{\mathbf{g}^T \mathbf{x}_{i+1} - g_k x_{i+1,k} + \sigma^2}$ with $v_k = x_{i,k}$. Substituting (16) into (7b), we obtain the user rate R_k

$$\begin{aligned} R_k &= - \int_{v_k(t)=1}^{v_k(t)=0} \frac{g_k}{\mathbf{g}^T \mathbf{v}(t) + \sigma^2} dv_k(t) \\ &= \sum_{i=0}^{n-1} \frac{g_k(x_{i,k} - x_{i+1,k})}{\mathbf{g}^T (\mathbf{x}_i - \mathbf{x}_{i+1})} \log \frac{\mathbf{g}^T \mathbf{x}_i + \sigma^2}{\mathbf{g}^T \mathbf{x}_{i+1} + \sigma^2}. \end{aligned} \quad (18)$$

To verify the path independence property of Theorems 1 and 2, we consider three different paths for (17) and evaluate the system performance and achievable rates via density evolution and bit error rate (BER) simulations.

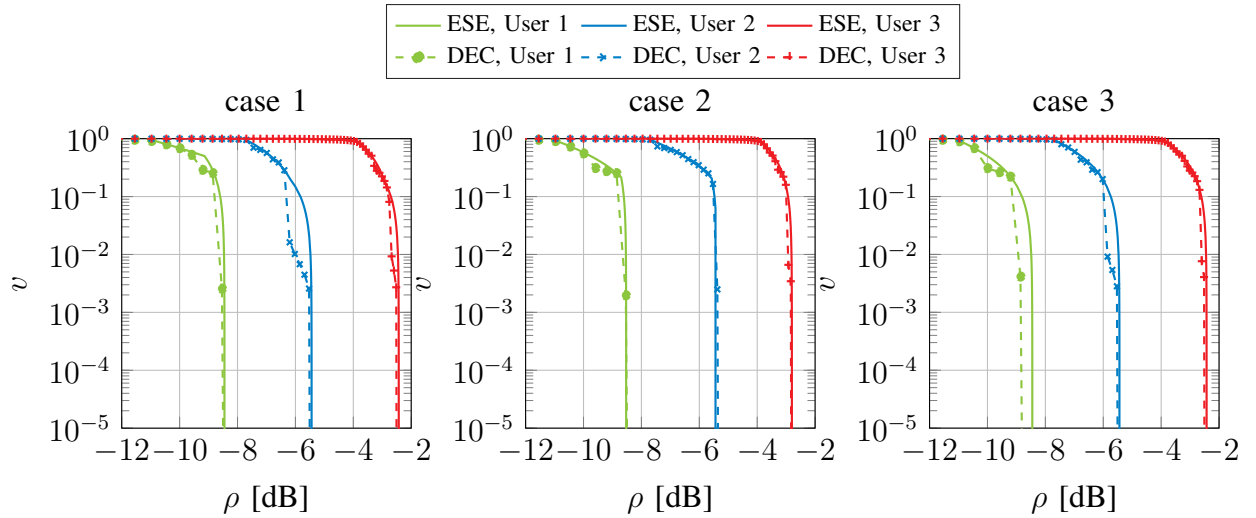


Fig. 5. ESE transfer function and the matching LDPC code transfer function for three different paths; the x-axis denotes the SNR of ESE and the y-axis denotes the MSE of the feedback from channel decoder; three users with QPSK and the power distribution $\mathbf{g} = [g_1, g_2, g_3]^T = [\frac{1}{7}, \frac{2}{7}, \frac{4}{7}]^T$ are considered.

1) *Case 1:* We do not specify any intermediate point $\{\mathbf{x}_i\}$, i.e., $n = 1$. The path is a straight line between the starting point $v(t = 0) = 1$ and the stop point $v(t = \infty) = 0$, as discussed in Sec. III-C. The ESE function for user k is given by

$$\rho_k = \frac{g_k}{(\mathbf{g}^T \mathbf{1} - g_k)v_k + \sigma^2}, v_k \in [0, 1]. \quad (19)$$

The rate for user k is proportional to its power g_k , i.e., $R_k = \frac{g_k}{\mathbf{g}^T \mathbf{1}} R_{\text{sum}}$. Thus, the corresponding rate tuple is $(R_1, R_2, R_3) = (\frac{1}{7}, \frac{2}{7}, \frac{4}{7})$. The transfer functions in (19) are depicted in the left most sub-figure in Fig. 5 for the three users, respectively.

2) *Case 2*: We construct a dedicated path to achieve an arbitrarily chosen rate tuple in the MAC region, e.g., $(R_1, R_2, R_3) = (0.15, 0.3, 0.55)$. To find a dedicated path, we search for $\{\mathbf{x}_i\}$ by solving K non-linear equations given by (18). Then, the ESE transfer functions can be obtained by substituting $\{\mathbf{x}_i\}$ into (17). If $n > 2$, there are $K(n-1)$ unknown variables $\{x_{i,k}\}$, which is larger than K . This potentially result in multiple solutions. It is noteworthy to mention that the variables $\{x_{i,k}\}$ are bounded in $[0, 1]$ and shall satisfy (15). We may fix some unknown variables $\{x_{i,k}\}$ and solve the K non-linear equations given by (18) to obtain remaining unknown variables. Usually, we can fix $K(n-2)$ unknown variables and have feasible solution for the remaining K unknown variables. Here, we consider a 3-segment path having intermediate points

$$\mathbf{x}_1 = [x_{1,1}, x_{1,2}, 0]^T \text{ and } \mathbf{x}_2 = [0, x_{2,2}, 0]^T. \quad (20)$$

Substituting (20) into (18), we obtain

$$\begin{aligned} 0.15 &= \frac{g_1(1-x_{1,1})}{1-g_1x_{1,1}-g_2x_{1,2}} \log_2 \frac{2}{g_1x_{1,1}+g_2x_{1,2}+1} \\ &\quad + \frac{g_1x_{1,1}}{g_1x_{1,1}+g_2(x_{1,2}-x_{2,2})} \log_2 \frac{g_1x_{1,1}+g_2x_{1,2}+1}{g_2x_{2,2}+1}, \\ 0.3 &= \frac{g_2(1-x_{1,2})}{1-g_1x_{1,1}-g_2x_{1,2}} \log_2 \frac{2}{g_1x_{1,1}+g_2x_{1,2}+1} \\ &\quad + \frac{g_2(x_{1,2}-x_{2,2})}{g_1x_{1,1}+g_2(x_{1,2}-x_{2,2})} \log_2 \frac{g_1x_{1,1}+g_2x_{1,2}+1}{g_2x_{2,2}+1} \\ &\quad + \log_2 (g_2x_{2,2}+1), \\ 0.55 &= \frac{g_3}{1-g_1x_{1,1}-g_2x_{1,2}} \log_2 \frac{2}{g_1x_{1,1}+g_2x_{1,2}+1}. \end{aligned} \quad (21)$$

Solving (21), we obtain one feasible solution given by $x_{1,1} = 0.2145, x_{1,2} = 0.2056, x_{2,2} = 0.0618$. Substituting the solution into (17), we can obtain the ESE functions. These transfer functions are depicted in the middle sub-figure of Fig. 5 for the three users, respectively.

3) *Case 3*: We randomly choose the intermediate points $\{\mathbf{x}_i\}$. Then, substituting the points into (17), we obtain the ESE transfer functions and subsequently compute the rate for each user using (18).

Here, we consider a piece-wise linear path with 2 segments by specifying an intermediate point arbitrarily, e.g., $\mathbf{x}_1 = [0.5, 0.2, 0.2]^T$. Substituting \mathbf{x}_1 into (17), we have the ESE functions

as

$$\begin{aligned}\rho_1 &= \begin{cases} \frac{g_1}{(g_2+g_3)0.4v_1+\sigma^2}, & 0 \leq v_1 \leq 0.5, \\ \frac{g_1}{g_2(1.6v_1-0.6)+g_3(1.6v_1-0.6)+\sigma^2}, & 0.5 \leq v_1 \leq 1, \end{cases} \\ \rho_2 &= \begin{cases} \frac{g_2}{g_1 2.5v_2+g_3v_2+\sigma^2}, & 0 \leq v_2 \leq 0.2, \\ \frac{g_2}{g_1(0.625v_2+0.375)+g_3v_2+\sigma^2}, & 0.2 \leq v_2 \leq 1, \end{cases} \\ \rho_3 &= \begin{cases} \frac{g_3}{g_1 2.5v_3+g_2v_3+\sigma^2}, & 0 \leq v_3 \leq 0.2, \\ \frac{g_3}{g_1(0.625v_3+0.375)+g_2v_3+\sigma^2}, & 0.2 \leq v_3 \leq 1. \end{cases}\end{aligned}$$

These transfer functions are depicted in the right most sub-figure of Fig. 5 for the three users, respectively. The achievable rates for each user, given in (22), can be obtained by substituting \mathbf{x}_1 into (18), see Tab. I.

$$\begin{aligned}R_1 &= \frac{g_1(1-0.5)}{g_1(1-0.5)+g_2(1-0.2)+g_3(1-0.2)} \log_2 \left(\frac{1+1}{g_1 \cdot 0.5 + g_2 \cdot 0.2 + g_3 \cdot 0.2 + 1} \right) \\ &\quad + \frac{g_1(0.5-0)}{g_1(0.5-0)+g_2(0.2-0)+g_3(0.2-0)} \log_2 (g_1 \cdot 0.5 + g_2 \cdot 0.2 + g_3 \cdot 0.2 + 1) = 0.157, \\ R_2 &= \frac{g_2(1-0.2)}{g_1(1-0.5)+g_2(1-0.2)+g_3(1-0.2)} \log_2 \left(\frac{1+1}{g_1 \cdot 0.5 + g_2 \cdot 0.2 + g_3 \cdot 0.2 + 1} \right) \\ &\quad + \frac{g_2(0.2-0)}{g_1(0.5-0)+g_2(0.2-0)+g_3(0.2-0)} \log_2 \left(\frac{g_1 \cdot 0.5 + g_2 \cdot 0.2 + g_3 \cdot 0.2 + 1}{0+1} \right) = 0.281, \\ R_3 &= \frac{g_3(1-0.2)}{g_1(1-0.5)+g_2(1-0.2)+g_3(1-0.2)} \log_2 \left(\frac{1+1}{g_1 \cdot 0.5 + g_2 \cdot 0.2 + g_3 \cdot 0.2 + 1} \right) \\ &\quad + \frac{g_3(0.2-0)}{g_1(0.5-0)+g_2(0.2-0)+g_3(0.2-0)} \log_2 \left(\frac{g_1 \cdot 0.5 + g_2 \cdot 0.2 + g_3 \cdot 0.2 + 1}{0+1} \right) = 0.562.\end{aligned}\tag{22}$$

B. LDPC code optimization

As the ESE functions are readily available, according to the matching condition, we optimize the degree profile of LDPC codes to match the ESE functions for user k , i.e.,

$$v_k = \psi_k(\rho_k) = \begin{cases} 1, & \rho_k \leq \rho_{k,\min}, \\ \phi_k^{-1}(\rho_k), & \rho_{k,\min} \leq \rho_k \leq \rho_{k,\max}, \\ 0, & \rho_k \geq \rho_{k,\max}, \end{cases}\tag{23}$$

Table I
CODE OPTIMIZATION RESULTS FOR THREE CASES

Case	Case 1, $R_{\text{sum}} = 1$			Case 2, $R_{\text{sum}} = 1$		
User	User 1	User 2	User 3	User 1	User 2	User 3
Power	$\frac{1}{7}$	$\frac{2}{7}$	$\frac{4}{7}$	$\frac{1}{7}$	$\frac{2}{7}$	$\frac{4}{7}$
Path	$[1, 1, 1] \rightarrow [0, 0, 0]$			$[1, 1, 1] \rightarrow [0.2145, 0.2056, 0] \rightarrow [0, 0.0618, 0] \rightarrow [0, 0, 0]$		
Target rate	0.1429	0.2857	0.5714	0.15	0.30	0.55
Check edge distribution	$\eta_3 = 1$	$\eta_4 = 1$	$\eta_5 = 1$	$\eta_3 = 1$	$\eta_4 = 1$	$\eta_5 = 1$
variable degree set $\{d_v\}$	{2:1:30, 35:5:50, 60:10:100}			{2:1:30, 35:5:50}		
Optimized variable edge distribution	$\lambda_2, 0.5239$ $\lambda_3, 0.2140$ $\lambda_7, 0.1627$ $\lambda_{30}, 0.0685$ $\lambda_{35}, 0.0309$	$\lambda_2, 0.3770$ $\lambda_3, 0.2168$ $\lambda_7, 0.0719$ $\lambda_8, 0.1577$ $\lambda_{40}, 0.1237$ $\lambda_{100}, 0.0529$	$\lambda_2, 0.3293$ $\lambda_3, 0.2351$ $\lambda_8, 0.2500$ $\lambda_{21}, 0.0654$ $\lambda_{22}, 0.0014$ $\lambda_{45}, 0.0258$ $\lambda_{50}, 0.0930$	$\lambda_2, 0.5234$ $\lambda_3, 0.2292$ $\lambda_7, 0.0896$ $\lambda_8, 0.0590$ $\lambda_{30}, 0.0708$ $\lambda_{35}, 0.0280$	$\lambda_2, 0.3779$ $\lambda_3, 0.2290$ $\lambda_7, 0.1431$ $\lambda_8, 0.0580$ $\lambda_{50}, 0.1920$	$\lambda_2, 0.3218$ $\lambda_3, 0.2273$ $\lambda_7, 0.0879$ $\lambda_8, 0.1654$ $\lambda_{20}, 0.0501$ $\lambda_{21}, 0.0335$ $\lambda_{50}, 0.1140$
Optimized rate	0.1467	0.3014	0.5707	0.1555	0.3154	0.5522
Case	Case 3, $R_{\text{sum}} = 1$			Case 2, $R_{\text{sum}} = 2$		
User	User 1	User 2	User 3	User 1 (1 Layer)	User 2 (2 Layers)	User 3 (4 Layers)
Power	$\frac{1}{7}$	$\frac{2}{7}$	$\frac{4}{7}$	$\frac{1}{7}$	$\frac{2}{7}$	$\frac{4}{7}$
Path	$[1, 1, 1] \rightarrow [0.5, 0.2, 0.2] \rightarrow [0, 0, 0]$			$[1, 1, 1] \rightarrow [0.9635, 0.7154, 0.0953] \rightarrow [0, 0, 0]$		
Target rate	0.157	0.281	0.562	0.4	0.7	0.9
Check edge distribution	$\eta_3 = 1$	$\eta_4 = 1$	$\eta_5 = 1$	$\eta_4 = 1$	$\eta_3 = 1$	$\eta_3 = 1$
variable degree set $\{d_v\}$	{2:1:30, 35:5:50}			{2:1:50, 60:10:100}		
Optimized variable edge distribution	$\lambda_2, 0.5250$ $\lambda_3, 0.2138$ $\lambda_6, 0.0978$ $\lambda_7, 0.0618$ $\lambda_{30}, 0.0604$ $\lambda_{35}, 0.0412$	$\lambda_2, 0.3788$ $\lambda_3, 0.1925$ $\lambda_6, 0.0763$ $\lambda_7, 0.1589$ $\lambda_{50}, 0.1935$	$\lambda_2, 0.3289$ $\lambda_3, 0.2277$ $\lambda_8, 0.1189$ $\lambda_9, 0.1747$ $\lambda_{45}, 0.1337$ $\lambda_{50}, 0.0161$	$\lambda_2, 0.4107$ $\lambda_3, 0.2398$ $\lambda_8, 0.1875$ $\lambda_9, 0.0339$ $\lambda_{10}, 0.0001$ $\lambda_{22}, 0.0001$ $\lambda_{35}, 0.0834$ $\lambda_{100}, 0.0445$	$\lambda_2, 0.6158$ $\lambda_3, 0.2261$ $\lambda_6, 0.0726$ $\lambda_7, 0.0413$ $\lambda_{44}, 0.0002$ $\lambda_{50}, 0.0440$	$\lambda_2, 0.5703$ $\lambda_3, 0.1699$ $\lambda_6, 0.1130$ $\lambda_7, 0.0713$ $\lambda_{16}, 0.0001$ $\lambda_{25}, 0.0277$ $\lambda_{26}, 0.0477$
Optimized rate	0.1588	0.2926	0.5608	0.4145	0.6844	0.8652

$$I_{E,V} = \sum_{i=1}^{d_{v,\max}} \lambda_i \cdot J \left(\sqrt{(i-1) \left[J^{-1} \left(1 - \sum_{j=1}^{d_{c,\max}} \eta_j \cdot J \left(\sqrt{j-1} \cdot J^{-1} (1 - I_{E,V}) \right) \right) \right]^2 + 4\rho} \right), \quad (27)$$

where $\phi_k^{-1}(\rho_k)$ is the inverse of the ESE function of user k and $\rho_{k,\min} = \frac{g_k}{\mathbf{g}^T \mathbf{1} - g_k + \sigma^2}$, $\rho_{k,\max} = \frac{g_k}{\sigma^2}$. Using the EXIT chart matching techniques [28], [32], [40], [41], the matching LDPC codes can be designed by properly choosing the degree distributions.

We basically follow the method described in [40, Appendix 5G] to design irregular LDPC codes given a target transfer function $v = \psi(\rho)$, where ρ is the *a priori* SNR and v , the decoder output, denotes the extrinsic variance. The difference is that we use mutual information instead of the mean of LLR to track the evolution process.

The asymptotic performance of an LDPC code ensemble can be specified by its variable node and check node edge distribution polynomials, namely

$$\lambda(x) = \sum_{i=1}^{d_{v,\max}} \lambda_i x^{i-1} \text{ and } \sum_{i=1}^{d_{c,\max}} \eta_i x^{i-1}, \quad (24)$$

where λ_i (resp., η_i) is the fraction of edges in the bipartite graph of the LDPC code connected to variable nodes (resp., check nodes) with degree i , and $d_{v,\max}$ (resp., $d_{c,\max}$) is the maximum variable node (resp., check node) degree. Moreover, we use the Gaussian approximation [42], i.e., (3a) and (4), to optimize the edge distributions for the sake of simplicity.

In [32], it is shown that the decoder characteristic for an LDPC code can be computed as

$$I_{E,V} = \sum_{i=1}^{d_{v,\max}} \lambda_i \cdot J \left(\sqrt{(i-1) [J^{-1}(I_{E,C})]^2 + 4\rho} \right), \quad (25)$$

$$I_{E,C} = 1 - \sum_{j=1}^{d_{c,\max}} \eta_j \cdot J \left(\sqrt{j-1} \cdot J^{-1}(1 - I_{E,V}) \right), \quad (26)$$

where $I_{E,V}$ (resp., $I_{E,C}$) is the extrinsic information from variable node (resp., check node) to check node (resp., variable node), ρ is the decoder input SNR, and the $J(\cdot)$ is defined by

$$J(\sigma_{ch}) = 1 - \int_{-\infty}^{\infty} \frac{e^{-\frac{(y-\sigma_{ch}^2/2)^2}{2\sigma_{ch}^2}}}{\sqrt{2\pi\sigma_{ch}^2}} \cdot \log_2 [1 + e^{-y}] dy,$$

its inverse function is further denoted by $J^{-1}(\cdot)$. Substituting (26) into (25), we have (27), where the LDPC code can be characterized by one single variable $I_{E,V}$. The degree optimization

$$\begin{aligned}
& \max_{\{\lambda_i\}} \sum_{i=1}^{d_{v,\max}} \frac{\lambda_i}{i} \\
& \text{s.t. } \sum_{i=1}^{d_{v,\max}} \lambda_i = 1, \\
& \sum_{i=1}^{d_{v,\max}} \lambda_i \cdot J \left(\sqrt{(i-1) \left[J^{-1} \left(1 - \sum_{j=1}^{d_{c,\max}} \eta_j \cdot J \left(\sqrt{j-1} \cdot J^{-1} (1 - I_{E,V}) \right) \right) \right]^2 + 4\rho} \right) > I_{E,V} \\
& \text{for } \forall 0 < \rho < \infty \text{ and } I_{E,V,\text{ini}}(\rho) \leq I_{E,V} \leq I_{E,V,\text{fin}}(\rho).
\end{aligned} \tag{28}$$

problem can be formulated in (28). The cost function in (28) is to maximize the code rate. Let $I_{E,V,\text{ini}}(\rho)$ be the initial extrinsic information given by the channel, which can be written as

$$\begin{aligned}
I_{E,V,\text{ini}}(\rho) &= \sum_{i=1}^{d_{v,\max}} \lambda_i \cdot J \left(\sqrt{(i-1) [J^{-1}(0)]^2 + 4\rho} \right) \\
&= J(2\sqrt{\rho}).
\end{aligned} \tag{29}$$

Let $I_{E,V,\text{fin}}(\rho)$ denote the extrinsic information upon convergence, which corresponds to an output extrinsic variance to the MUD $v = \psi(\rho)$, i.e., given ρ , $I_{E,V,\text{fin}}(\rho)$ should satisfy the following equation

$$\sum_{i=1}^{d_{v,\max}} \Lambda_i \cdot f_Q \left(\frac{i \cdot [J^{-1}(I_{E,C,\text{fin}})]^2}{4} \right) = \psi(\rho), \tag{30}$$

where f_Q is defined in (10), and

$$I_{E,C,\text{fin}} = 1 - \sum_{j=1}^{d_{c,\max}} \eta_j \cdot J \left(\sqrt{j-1} \cdot J^{-1}(1 - I_{E,V,\text{fin}}) \right)$$

is the converged message from check nodes to variable nodes. Furthermore, we define

$$\Lambda_i = \frac{\lambda_i/i}{\sum_{i=1}^{d_{v,\max}} \lambda_i/i}$$

as the fraction of variable node of degree i .

The optimization in (28) is a non-convex optimization. However, given $\{\Lambda_i\}$ and $\eta(x)$, the problem in (28) can be solved using standard linear programming. We use an iterative way to optimize the edge distribution $\lambda(x)$ with fixed $\eta(x)$ in Algorithm 1. In practice, Algorithm 1 is repeated for several check edge distributions $\eta(x)$ till a matching code is found.

Algorithm 1 Algorithm for LDPC Code Optimization in IDMA

Input: Target decoder transfer functions $v_k = \psi_k(\rho_k)$, check edge distribution $\eta_k(x)$, maximum trial T , threshold ϵ and maximum variable degree $d_{v,\max}$.

Output: The optimized variable edge distribution $\lambda^{(T)}(x)$.

```

1: Initialize  $\lambda^{(0)}(x) = x$ .
2: for  $t = 1$  to  $T$  do
3:   Solve (28) by linear programming to obtain  $\lambda^{(t)}(x)$ , where  $I_{E,V,\text{fin}}(\rho)$  in (28) is obtained
     by solving (30) using  $\lambda^{(t-1)}(x)$ .
4:   if  $1 - \frac{\sum_{i=1}^{d_{v,\max}} \lambda_i^{(t)} \lambda_i^{(t-1)}}{\sqrt{\left(\sum_{i=1}^{d_{v,\max}} (\lambda_i^{(t)})^2\right) \left(\sum_{i=1}^{d_{v,\max}} (\lambda_i^{(t-1)})^2\right)}} \leq \epsilon$  then
5:      $\lambda^{(T)}(x) = \lambda^{(t)}(x)$ .
6:   return  $\lambda^{(T)}(x)$ .
7:   end if
8: end for
9: return  $\lambda^{(T)}(x)$ .

```

C. Numerical Results

With Algorithm 1, if we use all variable degrees less than $d_{v,\max}$, the optimization can be quite slow. However, the optimized degree sequences are mostly comprised of a few small degrees. Therefore, we only use a subset of degrees less than $d_{v,\max}$ to run Algorithm 1 more efficiently. In the algorithm, we set $T = 100$ and $\epsilon = 0.001$ for all optimizations. The optimized results as well as other parameters are summarized in Table I. Fig. 5 shows the optimized LDPC DEC transfer functions (denoted by dashed lines). The DEC functions match enough well with the ESE functions.

After matching the degree distribution, we construct parity check matrices for BER simulations. The parity-check matrix of code-word length 10^5 for each user in each case is randomly generated and subsequently we remove the cycle-4 loops in the matrix by edge permutation [43]. Furthermore, we consider QPSK signaling in the simulation to verify that our Theorems work also well with finite alphabets, not only with Gaussian alphabets.

Fig. 6 shows the average BER performance for three users with matching codes along different decoding paths (denoted by solid lines, respectively), where we set a maximum iteration of 1000

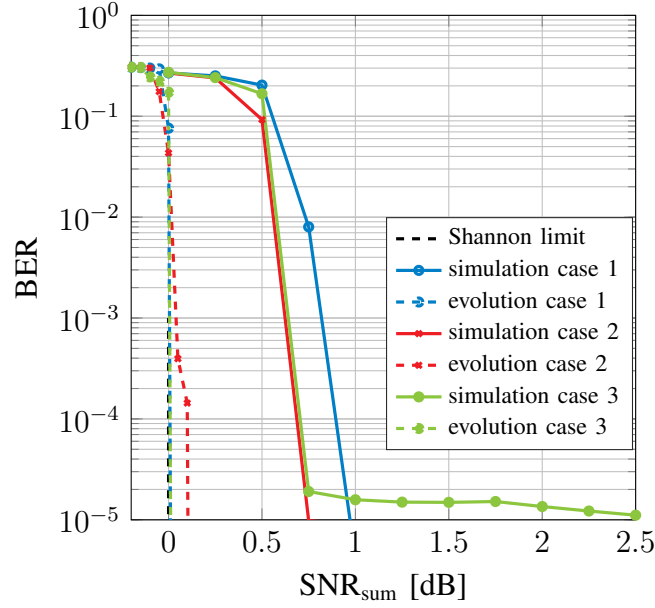


Fig. 6. BER curves and density evolution results for a three user MAC with matched codes; three different paths and QPSK signaling are considered.

between the ESE detector and the LDPC decoders. Moreover, the Shannon limit at the sum-rate $R_{\text{sum}} = 1$ along with the density evolution performance with optimized codes considering QPSK are provided. From the numerical results, we can conclude that

- the evolution thresholds for three cases with QPSK are close to the Gaussian capacity. The loss incurred by finite alphabets is negligible at the target sum-rate.
- Three cases have BER below 10^{-4} within 1 dB to the Shannon limit. The sum-rate capacity can be achieved for different paths also with QPSK signaling.
- For case 2, we computed a dedicated path to achieve an arbitrarily chosen rate tuple $(R_1, R_2, R_3) = (0.15, 0.3, 0.55)$. The numerical results also verified our path construction based on GA.

To further verify that the decoding path (or decoding trajectory $L(t)$) in the BER simulation is close to the desired path in the theory. We compare the decoding trajectories obtained via density evolution and BER simulation for three cases at the SNR $\text{SNR}_{\text{sum}} = 1$ dB, where all users can decode its signal with high probability. The evolution trajectories differ from the specified paths (discussed in Sec. V-A) mainly due to the different SNRs (the specified paths assume $\text{SNR}_{\text{sum}} = 0$ dB). We observe that the simulation trajectories are consistent with those of density evolution for all three cases. This further consolidates the path independence theorem, and provides numerical evidence for finite alphabet cases.

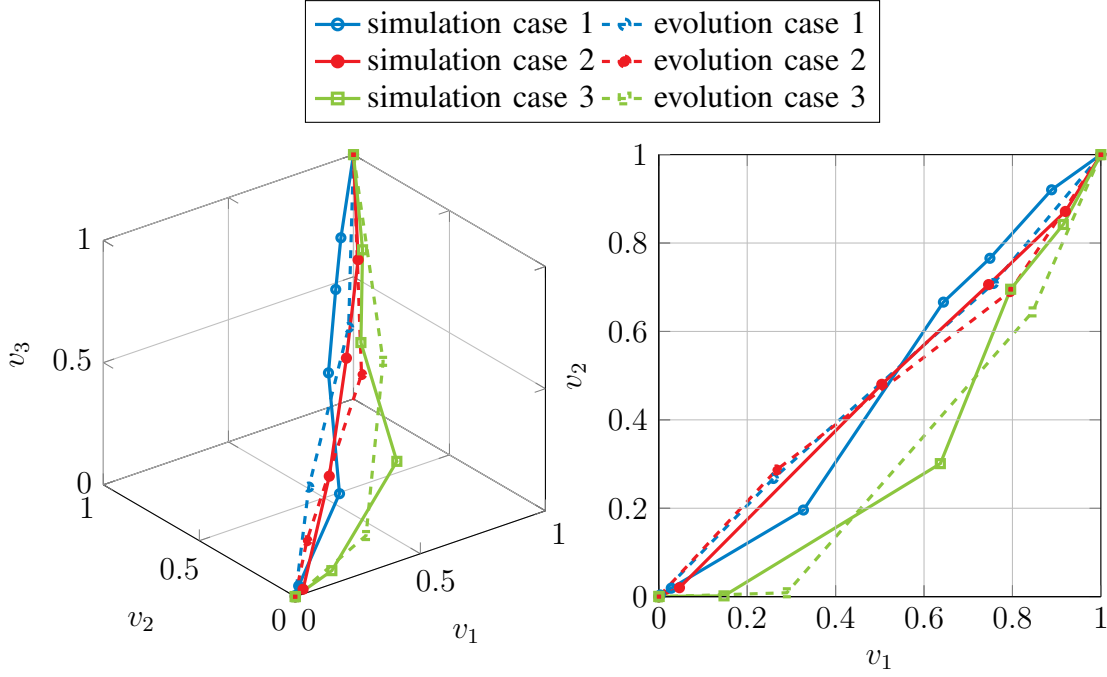


Fig. 7. Evolution and simulation trajectories for three cases at $\text{SNR}_{\text{sum}} = 1$ dB; Left: 3-D diagram for a trajectory (v_1, v_2, v_3) ; Right: Side view (v_1, v_2) of a trajectory.

D. High Rate

For scenarios where high rates per user is required, superposition coded modulation (SCM) [30] can be applied. We consider the case that the data layers in SCM are of the same power. Suppose that we have a K -user system with power allocation $[g_1, g_2, \dots, g_K]^T$. The decoding path $\mathbf{x}_0 \rightarrow \mathbf{x}_1 \rightarrow \dots \rightarrow \mathbf{x}_n$ is also specified. Then, we can convert this unequal power system into an equivalent equal power system as follows.

- Find a real number $g > 0$ such that $L_i = g_i/g$ is an integer for all i .
- Change each K -dimension point \mathbf{x}_i into a point \mathbf{x}'_i with dimension $L = \sum_{i=1}^K L_i$ as follows.

$$\mathbf{x}'_i = \left[\underbrace{x_{i,1}, \dots, x_{i,1}}_{L_1 \text{ copies}} \underbrace{x_{i,2}, \dots, x_{i,2}}_{L_2 \text{ copies}} \dots \underbrace{x_{i,K}, \dots, x_{i,K}}_{L_K \text{ copies}} \right].$$

- Finally, we have an equal power system with L virtual users each with power g and the decoding path is $\mathbf{x}'_0 \rightarrow \mathbf{x}'_1 \rightarrow \dots \rightarrow \mathbf{x}'_n$, where the original user i is the superposition of the virtual users with indices from $1 + \sum_{j=1}^{i-1} L_j$ to $\sum_{j=1}^i L_j$.

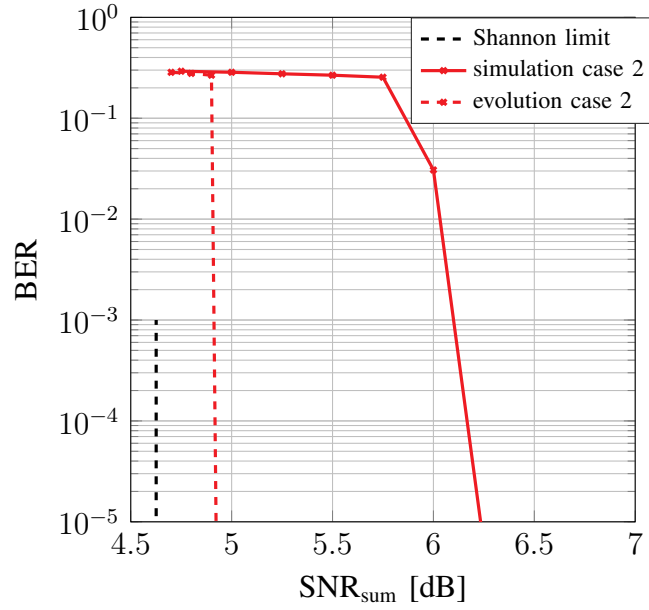


Fig. 8. BER and density evolution results for a three-user MAC with matched codes at the sum-rate $R_{\text{sum}} = 1.964$; SCM and QPSK signaling are considered.

By substituting the modified power allocation and path into (18), it is easy to find that the equal power system satisfies the requirement of the original K -user system.

Table I shows the optimized LDPC code for a targeted sum-rate of 2 for case 2, where the individual user rate is pre-defined and a dedicated decoding path is then specified to achieved that rate tuple. For the simplicity of code design, we applied SCM to each user. In particular, the to be transmitted data packet for user 2 and user 3 is divided into two and four independent data layers. By doing this, the three user MAC system is converted to a MAC system with seven “users”, each with the same transmit power. The main motivation for applying SCM is that the curve matching code design becomes difficult at high rate [16]. It may require rather complicated joint design of modulation and coding scheme for each user. Simulation and density evolution results are depicted in Fig. 8 for the most interesting case 2 (user rate is prescribed). Compared to the low-rate scenario in Fig. 6, the gap to Shannon-limit increases both for density evolution and simulation results at high rate (0.4 dB and 1.5 dB respectively). However, we conjecture that this gap can be reduced by imposing more data layers.

VI. CONCLUSION

It is proved under Gaussian approximation (GA) that the simple interleave-division multiple-access (IDMA), relying on a low-cost GA based multi-user detector (MUD), is capacity-achieving for general Gaussian multiple access channels (GMAC) with arbitrary number of users, power distribution and with single or multiple antennas. We show that IDMA with matching codes is capacity-achieving for arbitrary decoding path in the mean-square error (MSE) vector field. This property is further used to prove that IDMA achieves not only the sum-rate capacity, but the entire GMAC capacity region. The construction of capacity-achieving codes is also provided by establishing an area theorem for multi-user extrinsic information transfer (EXIT) chart. We provide numerical evidence supporting the GA and our achievable rate analysis.

APPENDIX A

PROOF OF (7b)

Let the SNR of ESE output $\rho_{k,\min}$, $\rho_{k,\max}$ as defined in (3d). Since the achievable rate formula in (7) requires the integration for the SNR ρ spanning $(0, \infty)$, we explicitly write the transfer function of the DEC as

$$v_k = \begin{cases} 1, & \rho \leq \rho_{k,\min} \\ \psi_k(\rho_k), & \rho_{k,\max} \leq \rho \leq \rho_{k,\min} \\ 0 & \rho \geq \rho_{k,\max} \end{cases}$$

We also assume that the matching condition in (6) holds. Then, the achievable rates can be expressed as

$$R_k = \int_{\rho_{k,\min}}^{\rho_{k,\max}} \frac{1}{\rho_k + v_k^{-1}} d\rho_k + \int_0^{\rho_{k,\min}} \frac{1}{\rho_k + 1} d\rho_k$$

Let ρ'_k be the first derivative of ρ_k with respect to v_k , we obtain

$$\begin{aligned} R_k &\stackrel{\rho'_k = \frac{d\rho_k}{dv_k}}{=} \int_{v_k=1}^{v_k=0} \frac{\rho'_k}{\rho_k + v_k^{-1}} dv_k + \int_0^{\rho_{k,\min}} \frac{1}{\rho_k + 1} d\rho_k \\ &= \int_1^0 \frac{\rho'_k - v_k^{-2} + v_k^{-2}}{\rho_k + v_k^{-1}} dv_k + \underbrace{\log(1 + \rho_{k,\min})}_{=w_0} \\ &= \left[\log(\rho_k + v_k^{-1}) + \int \frac{v_k^{-2}}{\rho_k + v_k^{-1}} dv_k \right]_{v_k=1}^{v_k=0} + w_0 \\ &= \left[\log(\rho_k + v_k^{-1}) + \int \left(v_k^{-1} - \frac{1}{\rho_k^{-1} + v_k} \right) dv_k \right]_{v_k=1}^{v_k=0} + w_0 \end{aligned}$$

Let $g_k = P_k |h_k|^2$ be the k th element of the vector \mathbf{g} and $\mathbf{v} = [v_1, v_2, \dots, v_K]$, we can express (3b) as $\rho_k = g_k / (\mathbf{g}^T \mathbf{v} - g_k v_k + \sigma^2)$ and obtain

$$\begin{aligned} R_k &\stackrel{(3a)}{=} \left[\log(\rho_k + v_k^{-1}) + \log v_k - \int_{v_k=1}^{v_k=0} \frac{g_k}{\mathbf{g}^T \mathbf{v} + \sigma^2} dv_k \right] + w_0 \\ &= \left[\log(\rho_k v_k + 1) - \int_{v_k=1}^{v_k=0} \frac{g_k}{\mathbf{g}^T \mathbf{v} + \sigma^2} dv_k \right] + w_0 \\ &= - \int_1^0 \frac{g_k}{\mathbf{g}^T \mathbf{v} + \sigma^2} dv_k \end{aligned}$$

where the last equality is due to $w_0 = \log(1 + \rho_{k,\min}) = \log(1 + \rho_k(v_k = 1))$.

APPENDIX B

PROOF OF THEOREM 2

The user rate $R_k = - \int_{v_k=1}^{v_k=0} \frac{g_k}{\mathbf{g}^T \mathbf{v} + \sigma^2} dv_k$ is a continuous and monotone decreasing function of \mathbf{v} . If v_k are unbounded, then R_k can take on any value with the single sum-rate constraint $\sum R_k \leq \log\left(\frac{\mathbf{g}^T \mathbf{1} + \sigma^2}{\sigma^2}\right)$. In other words, there exists at least one integration path which allows achieving an arbitrary point within the region determined by $\sum R_k \leq \log\left(\frac{\mathbf{g}^T \mathbf{1} + \sigma^2}{\sigma^2}\right)$. However, the value range of R_k is constrained by the fact that $0 \leq v_l \leq 1, \forall l$. Furthermore, the integrand $\frac{g_k}{\mathbf{g}^T \mathbf{v} + \sigma^2}$ is monotone decreasing with $v_l, \forall l \neq k$. Therefore, the maximum of the k th user rate R_k is attained when $v_l = 0, \forall l \neq k$, i.e.,

$$R_k \leq - \int_{v_k=1}^{v_k=0} \frac{g_k}{g_k v_k + \sigma^2} dv_k = \log\left(\frac{g_k + \sigma^2}{\sigma^2}\right).$$

Similarly, the following constraints can also be obtained

$$\begin{aligned} R_k + R_l &\leq \log\left(\frac{g_k + g_l + \sigma^2}{\sigma^2}\right), \forall k \neq l \\ R_k + R_l + R_m &\leq \log\left(\frac{g_k + g_l + g_m + \sigma^2}{\sigma^2}\right), \forall k \neq l \neq m \\ &\vdots \\ \sum R_k &\leq \log\left(\frac{\mathbf{g}^T \mathbf{1} + \sigma^2}{\sigma^2}\right) \end{aligned}$$

and these constraints constitute the MAC capacity region. Hence, for any point in rate region determined by the above constraints (or equivalently the K -user MAC capacity region), there exists at least an integration path constrained by $v_l, \forall l \neq k$ achieving that point.

REFERENCES

- [1] X. Wang, C. Liang, L. Ping, and S. ten Brink, "Achievable rate region for iterative multi-user detection via low-cost Gaussian approximation," in *to appear in Proc. IEEE Int. Symp. Inform. Theory*, 2019.
- [2] T. M. Cover and J. A. Thomas, *Elements of Information Theory*, 2nd ed. John Wiley & Sons, 2006.
- [3] A. E. Gamal and Y.-H. Kim, *Network Information Theory*. Cambridge University Press, 2011.
- [4] D. Tse and P. Viswanath, *Fundamentals of Wireless Communications*. Cambridge University Press, 2005.
- [5] Y. Hu and L. Ping, "Interleave-Division Multiple Access (IDMA)," in *Multiple Access Techniques for 5G Wireless Networks and Beyond*, M. Vaezi, Z. Ding, and H. V. Poor, Eds. Springer, 2019, ch. 13, pp. 417–449.
- [6] T. Richardson and R. Urbanke, *Modern Coding Theory*, 1st ed. Cambridge University Press, 2008.
- [7] C. Schlegel, R. Kempton, and P. Kota, "A novel random wireless packet multiple access method using CDMA," *IEEE Trans. Wireless Commun.*, vol. 5, no. 6, pp. 1362–1370, June 2006.
- [8] M. Jiang, J. Akhtman, and L. Hanzo, "Iterative joint channel estimation and multi-user detection for multiple-antenna aided ofdm systems," *IEEE Trans. Wireless Commun.*, vol. 6, no. 8, pp. 2904–2914, August 2007.
- [9] P. A. Hoeher, S. Badri-Hoeher, Wen Xu, and C. Krakowski, "Single-antenna co-channel interference cancellation for TDMA cellular radio systems," *IEEE Trans. Wireless Commun.*, vol. 12, no. 2, pp. 30–37, April 2005.
- [10] M. Zhao, Z. Shi, and M. C. Reed, "Iterative turbo channel estimation for OFDM system over rapid dispersive fading channel," *IEEE Trans. Wireless Commun.*, vol. 7, no. 8, pp. 3174–3184, August 2008.
- [11] S. ten Brink, "Exploiting the Chain Rule of Mutual Information for the Design of Iterative Decoding Schemes," in *Proc. 39th Annual Allerton Conf. on Comm., Control and Computing*, 2001.
- [12] T. J. Richardson, M. A. Shokrollahi, and R. L. Urbanke, "Design of capacity-approaching irregular low-density parity-check codes," *IEEE Trans. Inform. Theory*, vol. 47, no. 2, pp. 619–637, Feb 2001.
- [13] A. Ashikhmin, G. Kramer, and S. ten Brink, "Extrinsic information transfer functions: model and erasure channel properties," *IEEE Trans. Inform. Theory*, vol. 50, no. 11, pp. 2657–2673, Nov 2004.
- [14] K. Bhattad and K. R. Narayanan, "An MSE-Based Transfer Chart for Analyzing Iterative Decoding Schemes Using a Gaussian Approximation," *IEEE Trans. Inform. Theory*, vol. 53, no. 1, pp. 22–38, Jan 2007.
- [15] L. Ping, L. Liu, K. Wu, and W. K. Leung, "Interleave division multiple-access," *IEEE Trans. Wireless Commun.*, vol. 5, no. 4, pp. 938–947, April 2006.
- [16] Y. Hu, C. Liang, L. Liu, C. Yan, Y. Yuan, and L. Ping, "Interleave-division multiple access in high rate applications," *IEEE Comm. Letters*, 2018.
- [17] K. Li and X. Wang, "EXIT chart analysis of turbo multiuser detection," *IEEE Trans. Wireless Commun.*, vol. 4, no. 1, pp. 300–311, Jan 2005.
- [18] G. Song and J. Cheng, "Low-complexity coding scheme to approach multiple-access channel capacity," in *Proc. IEEE Int. Symp. on Inform. Theory*, June 2015, pp. 2106–2110.
- [19] L. Liu, Y. Chi, C. Yuen, Y. L. Guan, and Y. Li, "Capacity-achieving iterative LMMSE detection for MIMO-NOMA systems," *IEEE Trans. Signal Processing*, 2019.
- [20] X. Wang, S. Cammerer, and S. ten Brink, "Near Gaussian multiple access channel capacity detection and decoding," in *IEEE Int. Symp. on Turbo Codes Iterative Inform. Process. (ISTC)*, Dec 2018, pp. 1–5.
- [21] —, "Near-Capacity Detection and Decoding: Code Design for Dynamic User Loads in Gaussian Multiple Access Channels," *under review in IEEE Trans. Comm.*, 2019.
- [22] K. Li, X. Wang, and L. Ping, "Analysis and Optimization of Interleave-Division Multiple-Access Communication Systems," *IEEE Trans. Wireless Commun.*, vol. 6, no. 5, pp. 1973–1983, May 2007.

- [23] K. Kusume, G. Bauch, and W. Utschick, "IDMA vs. CDMA: Analysis and Comparison of Two Multiple Access Schemes," *IEEE Trans. Wireless Commun.*, vol. 11, no. 1, pp. 78–87, January 2012.
- [24] J. Song and Y. Shu, "On Construction of Rate-Compatible Raptor-Like QC-LDPC Code for Enhanced IDMA in 5G and Beyond," in *Proc. 10th Internat. Symp. Turbo Codes*, 2018.
- [25] P. Hammarberg, F. Rusek, and O. Edfors, "Channel estimation algorithms for OFDM-IDMA: Complexity and performance," *IEEE Trans. Wireless Commun.*, vol. 11, no. 5, pp. 1722–1732, May 2012.
- [26] T. Yang, J. Yuan, and Z. Shi, "Rate optimization for IDMA systems with iterative joint multi-user decoding," *IEEE Trans. Wireless Commun.*, vol. 8, no. 3, pp. 1148–1153, March 2009.
- [27] D. Guo, S. Shamai, and S. Verdú, "Mutual information and minimum mean-square error in Gaussian channels," *IEEE Trans. Inform. Theory*, vol. 51, no. 4, pp. 1261–1282, April 2005.
- [28] X. Yuan, L. Ping, C. Xu, and A. Kavcic, "Achievable Rates of MIMO Systems With Linear Precoding and Iterative LMMSE Detection," *IEEE Trans. Inform. Theory*, vol. 60, no. 11, pp. 7073–7089, Nov 2014.
- [29] S. ten Brink, "Convergence behavior of iteratively decoded parallel concatenated codes," *IEEE Trans. Commun.*, vol. 49, no. 10, pp. 1727–1737, Oct 2001.
- [30] L. Ping, J. Tong, X. Yuan, and Q. Guo, "Superposition coded modulation and iterative linear MMSE detection," *IEEE J. Sel. Areas Commun.*, vol. 27, no. 6, pp. 995–1004, August 2009.
- [31] T. Yang and J. Yuan, "Performance of iterative decoding for superposition modulation-based cooperative transmission," *IEEE Trans. Wireless Commun.*, vol. 9, no. 1, pp. 51–59, January 2010.
- [32] S. ten Brink, G. Kramer, and A. Ashikhmin, "Design of low-density parity-check codes for modulation and detection," *IEEE Trans. Commun.*, vol. 52, no. 4, pp. 670–678, April 2004.
- [33] D. Guo, Y. Wu, S. S. Shitz, and S. Verdú, "Estimation in Gaussian Noise: Properties of the Minimum Mean-Square Error," *IEEE Trans. Inform. Theory*, vol. 57, no. 4, pp. 2371–2385, April 2011.
- [34] Sae-Young Chung, G. D. Forney, T. J. Richardson, and R. Urbanke, "On the design of low-density parity-check codes within 0.0045 db of the Shannon limit," *IEEE Comm. Letters*, vol. 5, no. 2, pp. 58–60, Feb 2001.
- [35] X. Yuan, Q. Guo, X. Wang, and L. Ping, "Evolution analysis of low-cost iterative equalization in coded linear systems with cyclic prefixes," *IEEE J. Sel. Areas Commun.*, vol. 26, no. 2, pp. 301–310, February 2008.
- [36] S. Sharifi, A. K. Tanc, and T. M. Duman, "LDPC Code Design for the Two-User Gaussian Multiple Access Channel," *IEEE Trans. Wireless Commun.*, vol. 15, no. 4, pp. 2833–2844, April 2016.
- [37] A. Balatsoukas-Stimming and A. P. Liavas, "Design of LDPC Codes for the Unequal Power Two-User Gaussian Multiple Access Channel," *IEEE Wireless Comm. Letters*, pp. 1–1, 2018.
- [38] Y. Chi, L. Liu, G. Song, C. Yuen, Y. L. Guan, and Y. Li, "Practical MIMO-NOMA: Low Complexity and Capacity-Approaching Solution," *IEEE Trans. Wireless Commun.*, vol. 17, no. 9, pp. 6251–6264, Sep. 2018.
- [39] G. Song and J. Cheng, "Distance enumerator analysis for interleave-division multi-user codes," *IEEE Trans. Inform. Theory*, vol. 62, no. 7, pp. 4039–4053, July 2016.
- [40] X. Yuan, *Low-complexity iterative detection in coded linear systems*, Ph.D. dissertation, City University of Hong Kong, Hong Kong, China, 2008.
- [41] R. Y. S. Tee, R. G. Maunder, and L. Hanzo, "EXIT-chart aided near-capacity irregular bit-interleaved coded modulation design," *IEEE Trans. Wireless Commun.*, vol. 8, no. 1, pp. 32–37, Jan 2009.
- [42] S.-Y. Chung, T. Richardson, and R. Urbanke, "Analysis of sum-product decoding of low-density parity-check codes using a Gaussian approximation," *IEEE Trans. Inform. Theory*, vol. 47, no. 2, pp. 657–670, Feb. 2001.
- [43] J. A. McGowan and R. C. Williamson, "Loop removal from LDPC codes," in *Proc. IEEE Inform. Theory Workshop (ITW'03)*, Paris, France, 31 Mar. - 4 Apr. 2003, pp. 230–233.